

Organic Macromolecular High Dielectric Constant Materials: Synthesis, Characterization, and Applications

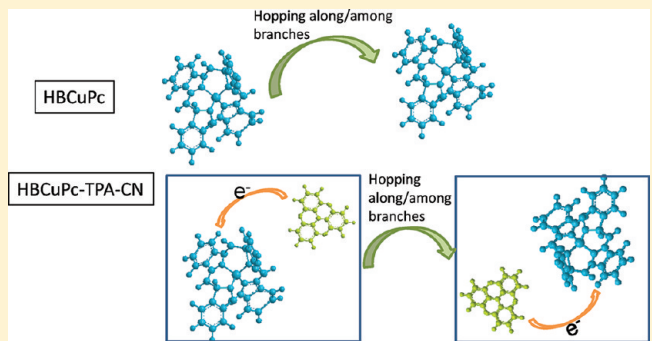
Meng Guo,[†] Teruaki Hayakawa,[‡] Masa-aki Kakimoto,[‡] and Theodore Goodson, III^{*,†}

[†]Department of Chemistry, University of Michigan, 930 North University, Ann Arbor, Michigan 48109, United States

[‡]Department of Organic and Polymeric Materials, Tokyo Institute of Technology, Tokyo 152-8550, Japan

 Supporting Information

ABSTRACT: Hyperbranched and dendritic architectures have been targeted for various applications such as sensing, drug delivery, optical limiting, and light harvesting. One interesting development in this area has focused on utilizing the existence of long-range delocalization in hyperbranched structures to achieve high dielectric constants. In this Feature Article, we will review the creation and development of this concept, and we highlight our recent research progress in this aspect. In particular, we discuss (1) synthetic methods for a particular group of hyperbranched polymers; (2) detailed optical and electronic characterization of this group of hyperbranched polymers, revealing the design criteria for achieving a good combination of high dielectric constant and minimum loss in such materials; and (3) the importance and potential applications of these materials.



of these materials.

1. INTRODUCTION

It is now clear that organic materials may be used in the development of high-speed capacitors and other energy storage devices.^{1–4} Indeed, high energy density and low loss capacitors powered at high frequency are essential electronic components for many electronic applications, which include pulsed lasers, implantable cardioverter defibrillators, hybrid cars, and display devices.^{1,2,4–8} Because the maximum energy density of a capacitor is determined by the product of the dielectric constant and the square of the breakdown field, high dielectric constant materials with high breakdown fields, minimum dielectric loss, and a low dielectric dispersion are strongly desirable in this rapidly developing technology. The traditional high dielectric constant materials for high energy density capacitors are ceramics.^{7,9–23} These materials can easily achieve very high dielectric constants at low frequency (1 Hz–10 kHz), especially with the advancement achieved in the material synthesis and new characterization techniques. Although it is true, because of better control in the size, phase, structure, and defects, that the dielectric properties of ceramics have been further improved, the dielectric performance of ceramic dielectrics are generally limited by the percolative nature of the materials, which will result in higher dielectric loss (>0.01), lower dielectric constant (<10) at high frequency, and a strong frequency dependence. In addition, these ceramic dielectrics are normally fragile and heavy, which prevents them from satisfying the demand from applications such as portable electronics.

The limitations of ceramic dielectrics mentioned above have led to the initial exploration of particular polymers as

candidates for high dielectric constant materials, such as polyaniline and polypropylene.^{24–29} One attractive property of polymer dielectrics is their high breakdown voltage. Other attributes such as the processing flexibility and potential lower cost add the attraction to this venture. However, one limitation concerning traditional polymers is their typically low dielectric constants (~3) in comparison with inorganic high dielectric materials. To compensate this shortcoming and take advantage of the high dielectric constant of ceramic dielectrics, considerable efforts have been given toward introducing inorganic fillers (e.g., Al, BaTiO₃) or conductive fillers (e.g., conductive polymers, carbon nanotubes) into the polymers.^{30–50} They are aimed at combining the desired properties from both the host polymer and organic/inorganic fillers. The host polymer matrixes are likely to be ferroelectric polymers, such as poly(vinylidene fluoride) (PVDF);⁵¹ polyimide (PI);³⁶ and epoxy.⁵² For example, Rao et al.⁵³ developed a high dielectric constant (~150 at 10 kHz) lead–magnesium niobate–lead titanate (PMN-PT)/BaTiO₃/epoxy nanocomposite with ceramic filler loading up to 85% by volume. The required high filler concentration that was necessary to achieve a higher dielectric constant results in a high dielectric loss and relatively low breakdown voltage in such polymer–ceramic composites. In addition, there are some technical barriers, such as poor dispersion of

Received: June 9, 2011

Revised: August 26, 2011

Published: September 27, 2011

the fillers in the polymer matrixes and poor compatibility with organic substrates.⁵⁴

One advantageous aspect of using conductive fillers is the ability to decrease the loading level in comparison to that of ceramics while obtaining a similar value for the dielectric constant. The effective dielectric constant of the composite system then follows the power law:⁵⁵

$$\frac{\kappa_{\text{eff}}}{\kappa_{\text{matrix}}} = |f_c - f|^{-s} \quad (1)$$

Here, κ_{eff} is the effective dielectric constant, κ_{matrix} is the dielectric constant of polymer matrix, f_c is the percolation threshold, f is the volume fraction of metal or inorganic fillers, and s is a scaling constant (~ 1), and the selection of its value depends on the material properties and phase connectivity between filler and polymer as well as the microstructure of the composite.^{38,56}

By approaching the percolation threshold (f_c), a very high dielectric constant is attainable. For instance, Dang et al.¹⁴ reported a large dielectric permittivity, ~ 400 at 100 Hz, in a functionalized carbon nanotube/poly(vinylidene fluoride) (PVDF) nanocomposite with a conductive filler loading of 8 vol %.³⁵ Despite the high dielectric constant, the dielectric loss was extremely high ($\tan \delta \sim 2$), and the dielectric properties of the composite were still constrained by the percolation limit. Therefore, an all-organic material with a high dielectric constant at high frequency with low loss has sparked great interest in the exploration of its usage for a variety of electronic and optical applications.^{3,4,57–60}

A good example is PVDF/poly(*p*-chloromethyl styrene) (PCMS) grafted copper phthalocyanine (CuPc) (PCMS-g-CuPc) organic composite, which showed a dielectric constant of 325 at 100 Hz due to the Maxwell–Wagner–Sillars polarization mechanism.⁵⁸ In addition, thiourea(TU)-graft-cyanoacrylate/PVDF composites possessed a dielectric constant ~ 54 up to 100 MHz.⁶⁰ However, their strong frequency dependence and large dielectric loss are still a major hurdle. For creating a superior material, for example, TU-graft-cyanoacrylate/PVDF composite had a loss tangent of ~ 0.03 . It will lead to a thermal effect and perhaps thermal failure of devices. Hence, it necessitates research on high dielectric constant and low dielectric loss all-organic materials.

We have performed an extensive investigation on the optical and electronic properties of particular dendritic structures, and the finding of an ultrafast delocalization process in many of these dendritic structures provides a novel avenue to create an organic capacitor with high energy density. In addition, due to the tunability of the properties of dendritic structures via precise control on the parameters such as the molecule size and weight, the morphology, the branching pattern, and the functional group, the scope of the potential applications in dendritic structures is expanding.

We initially started an investigation on a series of ion-doped hyperbranched polyaniline (HBPANI) polymers. An interesting finding was that the dielectric constant of these HBPANI polymers achieved ~ 200 at 1 MHz, two times larger than that of linear polyaniline.² The polaron hopping processes in these branched systems is dominated by the Marcus–Hush mechanism, and the hopping energy is <0.1 eV. The observed enhancement originates from a long-range polaron delocalization and a hyperelectronic polarization in these hyperbranched systems. Actually, the enhancement effect from the hyperelectronic polarization in polymeric systems was first observed by Pohl et al. several decades ago.^{59,61} They found the dielectric constant of polyacequinone radical polymers can go up to 240 000 at very low frequency. However,

a sharp decrease was observed at high frequency. The frequency dependence of the dielectric constant is similar to that of inorganic dielectric materials. In 2008, Zhang et al.⁶² observed a dielectric constant $\sim 1\ 200\ 000$ at 100 Hz in a polyacene quinine radical polymer synthesized by solid-state polymerization. The dielectric loss is huge (~ 30) but the frequency dependence was not reported. Inspired by these findings and on the basis of the understanding of polaron delocalization mechanism, we selected copper phthalocyanine as the core to build a series of hyperbranched polymers and investigate their dielectric and capacitance properties.

Recently, we demonstrated that a high dielectric constant and low dielectric loss are attainable by using polaron delocalization in hyperbranched polymer systems.^{1,2,63} For example, a very high dielectric constant (>46) and low dielectric loss (~ 0.004) were observed in a hyperbranched copper phthalocyanine system with very small dielectric dispersion.¹ The charge transfer mechanism for this impressive dielectric performance was related to a long-range polaron hopping process accompanied by strong intermolecular interactions in the branched systems. The high electron mobility ($\sim 10^{-4}\ \text{cm}^2\ \text{V}^{-1}\ \text{s}^{-1}$) in addition to the non-Arrhenius and Poole–Frenkel behavior observed from time-of-flight measurement provided a convincing proof for the strong and fast dielectric response found in this hyperbranched copper phthalocyanine system.⁶³ Moreover, ultrafast delocalization and electron hopping were demonstrated by femtosecond up-conversion fluorescence measurement, which were suggested to be able to enhance the dielectric response in hyperbranched systems in comparison with their linear analogues.^{2,63}

In this Feature Article, we discuss in detail the electronic, optical, and morphological studies on these hyperbranched copper phthalocyanine polymers. The synthesis as well as chemical characterization details will be referred to our previous publication, and only a short description will be provided here. This new class of high dielectric constant materials provides new avenues for the application and mechanistic studies of new capacitor devices.

2. EXPERIMENTAL SECTION

2.1. Materials. All reagents were purchased from Aldrich Chemical Co. and were used as received unless stated. The solvents of *N,N*-dimethylacetamide (DMAc), dimethyl sulfoxide (DMSO), and dimethylformamide (DMF) were dried with calcium hydride and distilled under reduced pressure.

2.2. Preparation of Films of the Hyperbranched Copper Phthalocyanine Polymer. A certain amount of hyperbranched copper phthalocyanine polymer powder was grinded in a mortar for 10 min, then the powder was poured into a vial filled with 0.5 mL of DMAc solution. The mixture was stirred on a hot plate for 10 h at room temperature. Heat was supplied for the first 3 h to help dissolve the polymer powder at a faster speed. The formed homogeneous gel solution from the mixture was sonicated for an extra 10 min to break any polymer aggregates. Both aluminum (Al) foil and indium tin oxide (ITO) glass were used as the substrates. For the ITO glass substrate, several steps of cleaning process were followed to avoid the contamination, and the film was coated on the conductive side of the ITO glass. The polymer films were prepared by both drop-casting and spin-coating methods. After drying in air overnight, the wet films were baked in the oven (temperature started from RT; increased by 20 °C after every 2 h; and finally stayed at 160 °C for 5 h) in vacuum at pressure (12 psi) to evaporate all the solvents.

2.3. Steady-State Spectroscopy Techniques. Ultraviolet (UV)–visible absorption spectra were recorded with an Agilent Technologies 8453 spectrophotometer. Steady-state fluorescence measurements were performed on a Fluomax-2 fluorimeter. The solvent for all spectroscopic measurement is DMAc.

2.4. Dielectric Measurement. Dielectric measurements were carried out with a 4284A HP LCR meter (20 Hz–1 MHz) connected with an HP 16451B dielectric fixture. A contact electrode method was used with Φ 5 mm guarded/guard electrodes. The capacitance (C_p) and dielectric loss ($\tan \delta$) were directly recorded from the LCR meter. The dielectric constant was determined by the equation:

$$K = \frac{C_p d}{\epsilon_0 A} \quad (2)$$

Here, ϵ_0 is the dielectric permittivity of the vacuum (8.85×10^{-12} F/m); A is the area of the electrode (m^2), and d is the thickness of the film (m). The film thickness was obtained by both scanning electron microscopy (SEM) cross section measurement and Dektak surface profiler, and the results were in good agreement with each other.



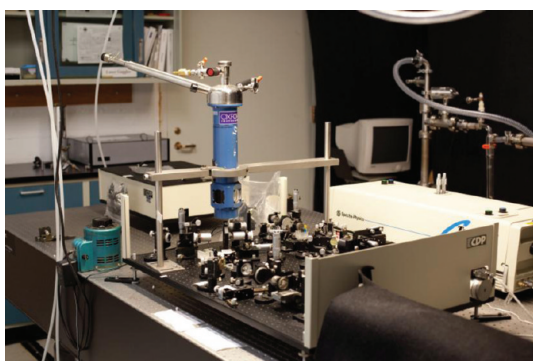
2.5. Time-Resolved Fluorescence Decay and Anisotropy Measurements. Time-resolved polarized fluorescence measurements were carried out on a femtosecond fluorescence up-conversion setup. The detailed description of the setup has been provided elsewhere.^{64,65} In brief, the hyperbranched copper phthalocyanine polymer/DMAc solution was excited with frequency-doubled light from a mode-locked Ti-sapphire laser with a pulse width of ~55 fs at a wavelength of 820 nm. The polarization of the excitation beam for the anisotropy measurements was controlled with a Berek compensator. The sample cell was 1 mm thick and was held in a rotating holder to avoid possible photodegradation and other accumulative effects. The fluorescence emitted from the sample was collected with a chromatic lens and directed parallel or perpendicular to a nonlinear crystal of β -barium borate. After passing through a motorized optical delay, the rest of the fundamental light mixed with the emission from the sample in another nonlinear crystal to generate a sum frequency signal. This up-conversion signal was dispersed using a monochromator and detected using a photomultiplier tube (R 1527P, Hamamatsu City, Japan).

The measured fluorescence decay was calculated according to the expression

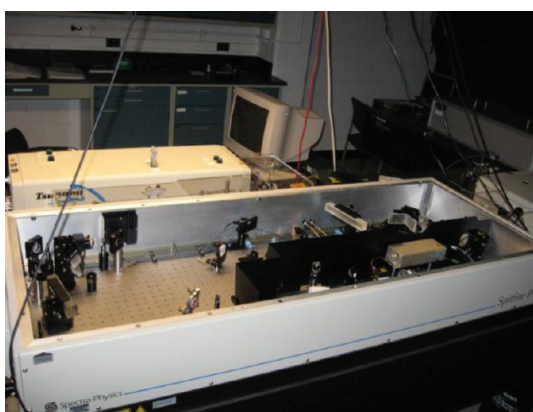
$$r(t) = \frac{I_{\text{par}} - GI_{\text{per}}}{I_{\text{par}} + 2GI_{\text{per}}} \quad (3)$$

Here, I_{par} and I_{per} are the intensities of fluorescence polarized perpendicular and parallel to the polarization of excited light,

respectively. The G factor accounts for the varying sensitivities for the detection of emission at perpendicular and parallel polarization configurations and is 1.01 in our case. The standard for obtaining the G factor in the experiment was the perylene dissolved in cyclohexane solution.

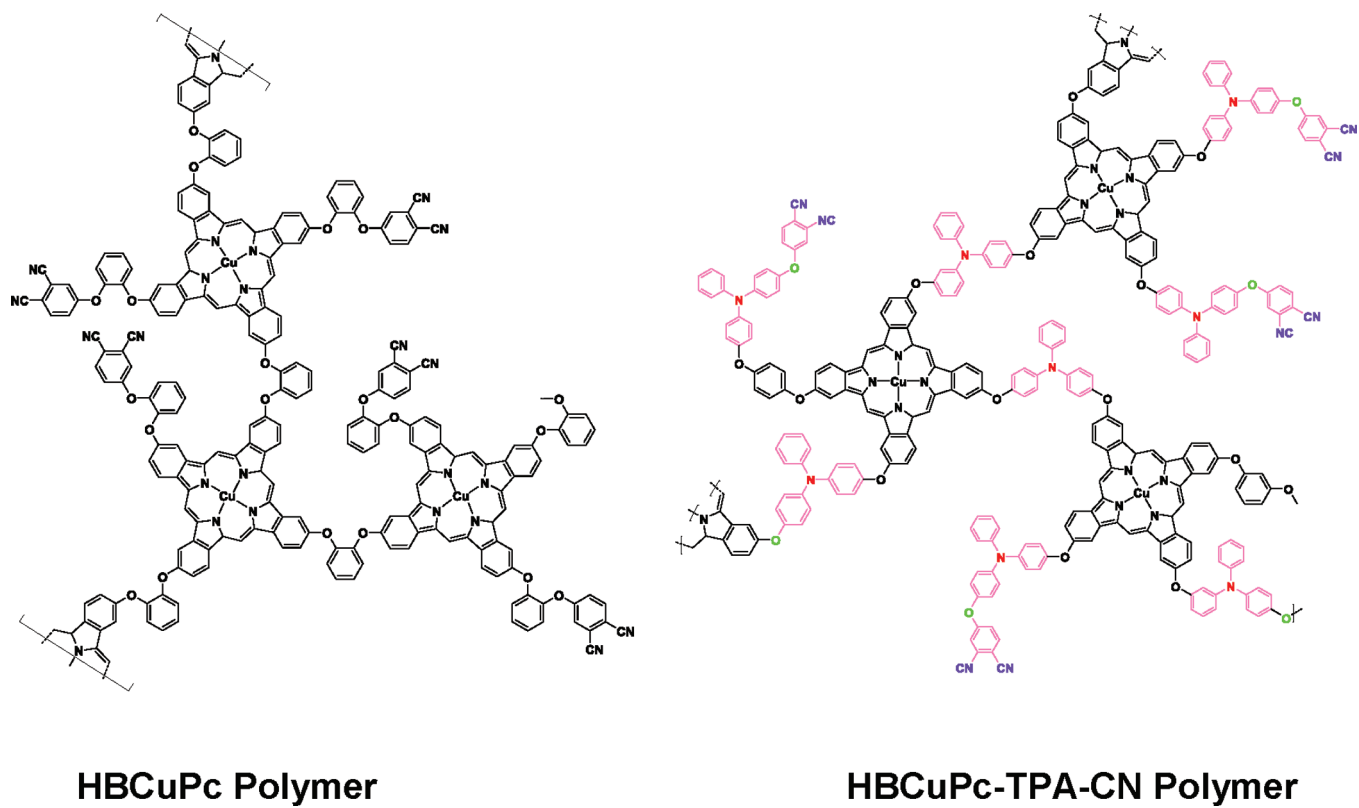


2.6. Pump Probe Transient Absorption Measurements. Transient absorption measurements were used to investigate the excited state dynamics of hyperbranched phthalocyanine polymers at different excitation wavelengths, and the description of the system has been provided elsewhere.⁶⁶ Briefly, the pump beam was produced by the OPA-800C. The pump beams used in the present investigation were obtained from the fourth harmonic of the idler beams and were focused onto the sample cuvette. The probe beam was delayed with a motion controller operated by computer and then focused into a 2 mm sapphire plate to generate white light continuum. The white light was then overlapped with the pump beam in a 2 mm quartz cuvette containing the sample, and the change in the absorbance for the signal was collected by a CCD detector (Ocean Optics). Data acquisition was controlled by the software from Ultrafast Systems Inc. For this measurement, we used a pump power of 250 nJ per pulse, and the kinetics was found to be independent of pump power for all the investigated phthalocyanine polymers. Magic angle polarization was maintained between the pump and probe using a wave plate. The pulse duration was obtained by fitting the solvent response, which was 130 fs. The sample was stirred with a rotating magnetic stirrer, and no photodegradation of the sample has been observed.



3. RESULTS AND DISCUSSION

3.1. Synthesis. Hyperbranched polymers have attracted great interest due to the unique chemical and physical properties in

Scheme 1. Illustration of the Structure of HBCuPc (left) and HBCuPc-TPA-CN (right) Polymers

comparison with linear polymers: (1) low solution viscosity and improved solubility in organic solvents, (2) improved thermal stability, and (3) enhanced terminal end group functionality due to the irregular and dense branching structure.^{67–69} Several approaches have been developed and reported in the past to synthesize a wide variety of hyperbranched macromolecules, such as the step growth approach^{70–72} and chain growth approach.^{73,74} Excellent reviews on the synthesis and characterization of hyperbranched polymers have been published in the literature.^{67,75–79} Here, we focus only on the synthesis of the particular group of hyperbranched phthalocyanine polymers, which were prepared by convenient one-pot polymerization from AB_x monomers. Scheme 1 illustrates the example structures of the HBCuPc polymer and HBCuPc-TPA-CN polymer. Both polymers were synthesized by a copper-fusion method. The detailed description of the copper fusion method as well as the synthesis and chemical characterization for HBCuPc polymer have been dealt with elsewhere.^{1,80} Here, we only briefly give an example of the synthesis of the HBCuPc-TPA-CN polymer. The HBCuPc-TPA-CN polymer was synthesized by a copper fusion method,^{80,81} too, through the polymerization reaction of bis(3,4-dicyanophenoxy)phenylamine and copper(I) chloride.

The synthesis of bis-(3,4-dicyanophenoxy)phenylamine monomer is summarized in Scheme 2. Briefly, aniline was first coupled with 4-iodoanisole using copper(I) chloride, potassium hydroxide, and 1,10-phenanthroline to produce bis(4-methoxyphenyl)phenylamine (**1**), followed by the demethylation reaction by Br_3 to yield bis(4-hydroxyphenyl)phenylamine (**2**). Then, the coupling reaction of bis(4-hydroxyphenyl)phenylamine and 4-nitrophthalonitrile was carried out using potassium

carbonate in DMSO to form bis((3,4-dicyanophenoxy)phenyl)phenylamine. For the final step, to a flask, 4 g (14.42 mmol) of bis(4-hydroxyphenyl)phenylamine, 6.24 g (36.06 mmol) of 4-nitrophthalonitrile, and 9.97 g (72.12 mmol) of K_2CO_3 were dissolved in 80 mL of DMSO at room temperature under nitrogen atmosphere and stirred for 48 h. Then, the mixture solution was cooled to 0 °C, and water was added to generate the solid. The precipitate was collected by filtration and rinsed with cold methanol. The precipitate was purified by recrystallization with methanol and ethyl acetate to generate 5.52 g (72%) of bis((3,4-dicyanophenoxy)phenyl)phenylamine as a yellowish powder.

Following this, a mixture of 2 g (3.78 mmol) of bis((3,4-dicyanophenoxy)phenyl)phenylamine and 112.17 mg (1.13 mmol) of copper(I) chloride was added to the flask and dissolved in 5 mL of DMAc at 160 °C under nitrogen atmosphere. The mixture was stirred for 8 h before pouring into 1000 mL of water. The precipitate was collected by filtration, dried under vacuum, dispersed in methanol, and refluxed for 6 h. Then it was filtered, dried under vacuum, dissolved in DMAc, and stirred for 6 h. After the filtration, the filtrate was poured into methanol, and the precipitated polymer was filtered off and dried under vacuum. A 780 mg portion of HB-CuPc-TPA was obtained as a dark blue solid. The final structure was characterized by 1H NMR, FT-IR, and DI-mass spectra. The HBCuPc-TPA-CN polymers with varying molecular weight were synthesized. The sample under this investigation has a molecular weight (M_w) of 20 000.

The detailed characterization result of both the monomer and the HBCuPc-TPA-CN polymer using 1H NMR, ^{13}C NMR, FT-IR and DI-mass spectra are provided in the Supporting Information.

Scheme 2. Synthesis of Bis((3,4-dicyanophenoxy)phenyl)-phenylamine Monomer

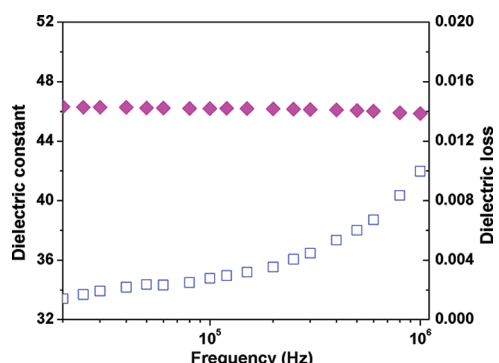
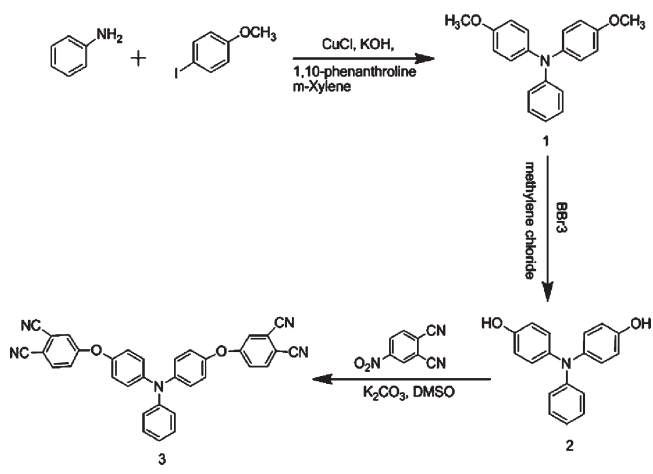


Figure 1. Dielectric constant and dielectric loss curves of HBCuPc polymer pellet with a thickness of $76\ \mu\text{m}$. Reproduced from ref 1.

3.2. Dielectric Response. The dielectric property is the key characteristic of a capacitor. Here, we want to re-emphasize the advantage of our strategy lies in the good combination of high dielectric constant and low dielectric loss at the high frequency domain (kHz–MHz). Figure 1 shows the dielectric response (dielectric constant, dielectric loss) dependence on the frequency of the HBCuPc polymer. One distinctive characteristic is the negligible frequency dependence of the dielectric constant over the wide frequency domain ($10\ \text{kHz}$ – $1\ \text{MHz}$). For other reported CuPc complexes, generally, one would expect a dramatic drop in dielectric constant with at least 3 orders of magnitude over the same frequency domain. Along with the improvement in the dielectric constant, the dielectric loss has dropped significantly, too.

To probe the importance of the morphology of the system once fabricated in the solid-state, we also prepared dielectric films varying in thickness and concentration of the HBCuPc polymers. Shown in Figure 2 is the frequency dependence of the dielectric response of a casted HBCuPc polymer film with a thickness around $10\ \mu\text{m}$. A very small dispersion was observed, and a very small dielectric loss (on the order of 0.001) was obtained at high frequency (MHz). The dielectric constant was close to ~ 15 at 1 MHz.

As part of many efforts to optimize the design of the hyperbranched copper phthalocyanine polymer as well as

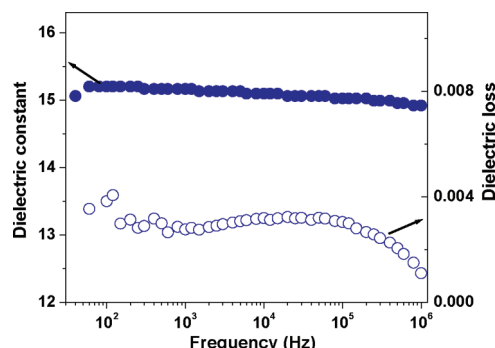


Figure 2. Dielectric constant and dielectric loss curves of HBCuPc polymer film with a thickness of $10\ \mu\text{m}$. Reproduced from ref 1.

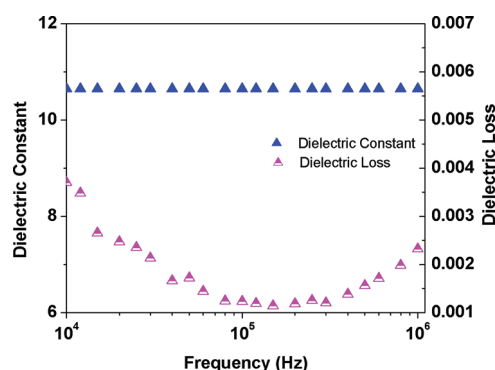


Figure 3. Dielectric constant and dielectric loss curves of HBCuPc-TPA-CN polymer pristine film with a thickness of $10\ \mu\text{m}$.

improve its processability, the HBCuPc-TPA-CN polymer was synthesized, and the dielectric behavior of the HBCuPc-TPA-CN polymer cast films with different thicknesses (1 – $10\ \mu\text{m}$) and substrates was probed and compared. A very good reproducibility has been shown in the dielectric test results because no visible degradation in the performance was observed in a 4 year testing window. One important characteristic of these films is the excellent thermal stability at room temperature in air. The ongoing work includes the longer term thermal stability test and the performance evaluation of the film resistance to harsh environments (high temperature, acid medium et al.). Figure 3 shows the dielectric properties of the HBCuPc-TPA-CN polymer film with a thickness of $\sim 10\ \mu\text{m}$ as a function of the frequency. It clearly shows a weak frequency dependence of the dielectric constant in the HBCuPc-TPA-CN polymer, following a trend similar to that of the previous reported HBCuPc polymer film.¹ The dielectric constant of the HBCuPc-TPA-CN polymer film at 1 MHz was ~ 11 , which is a distinct improvement over previously investigated triphenylamine-based polyamides (~ 3 – 4) and CuPc monomer (~ 5) systems.^{7,82} The enhancement may be due to the ultrafast delocalization of the rigid macrocycles of CuPc rings within the hyperbranched architecture. In addition, the increased delocalization length in hyperbranched polymer in relation to that of the monomer may play an important role, too.

In the original design criteria, we were hoping to gain an increase in the dielectric constant of the HBCuPc-TPA-CN polymer through the extension of the conjugation length.

However, possibly due to the inhibition of the face-to-face packing of CuPc rings because of the tetrahedral shape of triphenylamine moiety, a relatively lower dielectric constant was actually obtained in the HBCuPc-TPA-CN polymer film. In addition, we observed the existence of charge transfer (CT) states in the HBCuPc-TPA-CN polymer from pump–probe transient absorption measurement, which will be discussed in detail later. These additional CT states play some role in influencing the formation pathways and rates for singlet and triplets excitons in the hyperbranched system,^{83–86} which has been considered to vary the rate of the dominating polaron hopping process. Furthermore, the formation of a CT complex between the TPA donor and the CuPc acceptor may result in a low polaron hopping activation energy and an increase in the effective hopping distance. As expected, the solubility of the HBCuPc-TPA-CN polymer in solvents such as DMAc, DMSO, and DMF has been greatly enhanced. This will help to ease the film fabrication process and later on benefit the device volume manufacturing process.

The dielectric loss decreased sharply from 0.028 at 1 kHz with the increase in the frequency, which demonstrates a strong ionic polarization feature in the system and is mainly due to the formation of a CT complex between the TPA and the CuPc. Then the dielectric loss curve reached the bottom at 100 kHz with a value ~0.001 (Figure 3). In addition, the exciton traps induced by the TPA donor may immobilize a considerable number of charge carriers and cause a delay in the response to the rearrangement of the dipole orientation at low frequencies.

Within the frequency ranges between 100 kHz and 1 MHz, the dielectric loss dissipation was very small and reached a value of 0.0025 at 1 MHz, close to that of the HBCuPc casting film. The low dielectric loss at this region corresponds to the increased disorder in the amorphous state. The lower dielectric loss is very favorable for high performance devices operating at high frequency, where high efficiency and low noise are required. The low dielectric loss found in both hyperbranched phthalocyanine systems suggests that it is an intrinsic property of such hyperbranched systems, pointing out an effective way to lower the dielectric loss in polymeric dielectric materials, especially for high frequency applications.

As a part summary, the concept of utilizing the long delocalization in hyperbranched architecture to achieve both high dielectric constant and low dielectric loss is feasible and promising for next generation high energy density capacitor applications.

3.3. Charge Transfer Mechanisms. An effective mechanism of transport of charge carriers in the hyperbranched polymer system will enable the improvement in its dielectric response. A better understanding of the operative charge transfer mechanisms in the hyperbranched polymer system is crucial to the development of organic high dielectric materials. The AC electrical properties of the HBCuPc-TPA-CN polymer may be able to provide important information about the electronic conduction processes, which can be obtained by analyzing the frequency exponent predicated by different theoretical models on the basis of polaron hopping and quantum mechanical tunneling.^{87–89} In general, $\sigma \propto \omega^s$ dependence is shown in CuPc-based materials for low temperatures and high frequencies, which is in accordance with the hopping conduction. For example, Sadaoka and Sakai observed a power law conductivity dependence ($\sigma \propto \omega^s$) not only for compressed powders but also for thin films of CuPc monomers and concluded that the hopping was a major conduction process in CuPc.⁸⁹ Vidadi et al. also

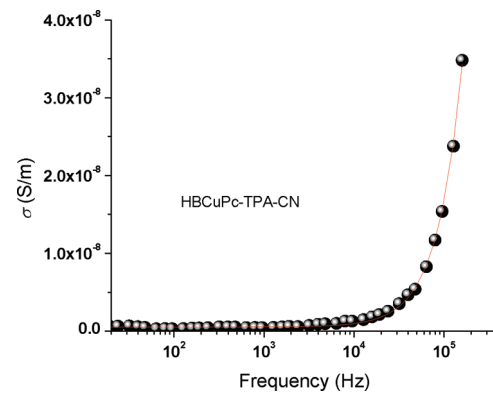


Figure 4. AC conductance of the HBCuPc-TPA-CN film.

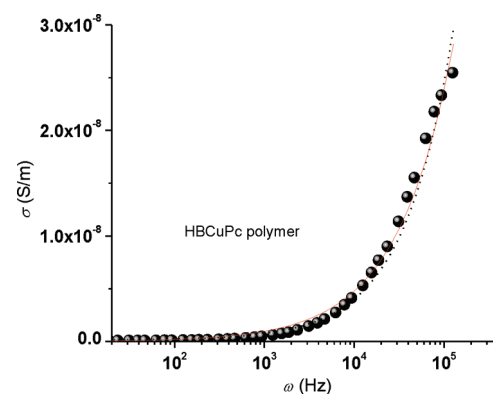


Figure 5. AC conductance of the HBCuPc polymer film.

suggested for a CuPc film that the charge carrier transport was dominated by hopping in the low temperature and high frequency region.⁹⁰ Although AC measurements have been carried out in various phthalocyanine-based monomers and polymers, few reports are available for hyperbranched or dendritic CuPc macromolecules. Therefore, in this work, we are going to carefully examine the AC conductance versus frequency relationship of the HBCuPc-TPA-CN polymer films (Figure 4). By drawing the comparison to that of the HBCuPc polymer film (Figure 5), the effect of the polymer structure and composition on the charge transport process will be known. It will be essential for further development in this area. For our case, superlinear power law dependence was found from the fitting of the AC conductance ($\sigma_{AC} = A + B\omega^s$):

$$\sigma = 5.5895 \times 10^{-10} + 1.9418 \times 10^{-16} \omega^{1.58} \quad (4)$$

A value of $s = 1.58$ for the exponent of the $\sigma(\omega)$ function was determined for the HBCuPc-TPA-CN polymer films at the frequency range (20 Hz–1 MHz), indicating that the polaron hopping conduction is the dominating charge carrier transport mechanism operative in the HBCuPc-TPA-CN polymer film. It is clearly seen that no visible change in the conductivity with frequency up to 10 kHz, which is typical for hopping conduction. But more charge carriers may be available to “hop” by tunneling upon further increase in the frequency, which explains the increase in the bulk conductivity above 10 kHz. Hence, both polaron hopping and polaron tunneling mechanisms are operative in the HBCuPc-TPA-CN polymer film.

In the literature, very few results of such superlinear power law dependence were reported for CuPc-based films. This is the first time that an $s > 1$ dependence was found in the HBCuPc-TPA-CN polymer film for a wider frequency range (20 Hz–1 MHz) at room temperature in CuPc-based polymer films. Others have reported that an s of 1.75 for the $\sigma(\omega)$ function exponent was determined at frequencies of 10 kHz–1 MHz in CuPc films. Such behavior was normally observed in semiconducting glasses (e.g., $0.3[x\text{Li}_2\text{O} \cdot (1-x)\text{Li}_2\text{O}]0.7\text{B}_2\text{O}_3$).

In Figure 5, the AC conductance of the HBCuPc polymer film is shown for comparison. A typical $\sigma \propto \omega^s$ dependence was followed, and value of $s \sim 0.7$ was determined at room temperature for the same frequency range, indicative of polaron hopping conduction.¹ The variance in the charge transport process between two hyperbranched CuPc polymer films may provide important information on the interactions within the macromolecule and explain the difference in their dielectric performance discussed earlier. Due to the introduction of electron rich TPA units, a possible existence of a stronger dipole orientation in this HBCuPc-TPA-CN polymer will result in a larger AC conductance, especially at high frequency domain.⁹¹ The formation of $\text{CuPc}^{+}-\text{TPA}^{+}$ charge transfer states with stronger electron coupling hence contributed to a slightly higher AC conductance in the HBCuPc-TPA-CN polymer. It also provides evidence for the higher dielectric loss we observed, especially at the lower frequency range, and the relatively lower dielectric constant may indicate an interruption of long-range delocalization along the branch in the HBCuPc-TPA-CN system as compared with that in the HBCuPc system.

$$\sigma = 7.8441 \times 10^{-12} \omega^{0.696} \quad (5)$$

It is important to note that the dispersion of the dielectric constant as well as the value of loss tangent remain very low in both systems, especially at high frequencies (kHz–MHz). Therefore, they are very promising for energy storage applications in which a quick burst of power is needed. The dielectric behavior we observed on both hyperbranched CuPc polymers supports the proposed concept of utilizing the long-range delocalization to enhance the dielectric response in polymeric materials, especially in terms of the minimum dielectric loss. However, the formation of the CT complex will influence the disorder and delocalization length in the system, resulting in a change on polaronic transport and the dielectric response.^{2,92,93} Martens and Brom have suggested that the electronic delocalization is dominated by an intergrain charge transfer process.⁹⁴ With the possibility to form more charge transfer states, more delocalization sites will be available in the HBCuPc-TPA-CN polymer. However, if there are some defects along the boundary between the donor and the acceptor, the enhancement in the dielectric constant may be limited.

To evaluate the dielectric performance in such hyperbranched system and optimize the film fabrication processes, other casting films of HBCuPc and HBCuPc-TPA-CN polymer were prepared by varying the solvent and the substrate. The thickness effect has been eliminated by keeping the films at the same thickness ($\sim 10 \mu\text{m}$). We found that the films prepared from sonicated solutions have smaller dielectric dispersion while maintaining a similar dielectric performance in general. The alleviated dielectric dispersion may be related to the reduced amount of crystalline nano domains of polymer particle and induced disorder in this system. The films cast on ITO glass showed a much stronger

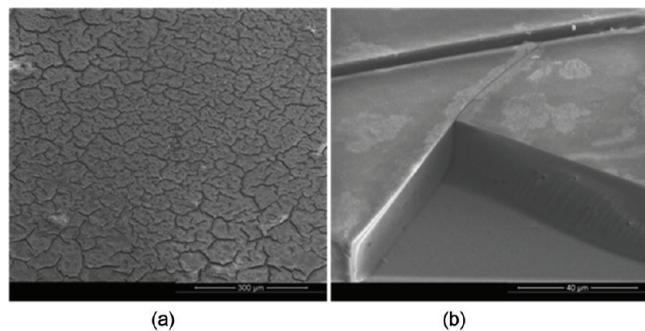


Figure 6. SEM image of the surface of HBCuPc polymer film on (a) Al foil; (b) ITO glass.

ionic polarization in the dielectric loss spectrum, which indicates the formation of the polymer/tin oxide interface. The SEM cross section also confirmed the existence of such an interface, as shown in Figure 6. A honeycomb surface was observed on the film coated on Al foil, whereas a more homogeneous, well distributed, 3D pie surface was seen with the substrate of ITO glass.

In addition, a clear HBCuPc polymer/Indium tin oxide interface was observed, which results in a larger conductance, dielectric loss and dielectric dispersion. In addition, from the dielectric loss spectrum, a dielectric loss peak indicates the interface polarization was occurring in this dielectric film; therefore, a stronger dielectric dispersion and larger dielectric loss were observed. It suggests that the substrate is important in the dielectric performance, too.

3.4. Charge Transport Mechanisms. The optical properties of CuPc have been intensively studied due to their potential electronic and optical applications, such as photovoltaic cells, optical limiting, and photosensors. However, only a limited number of reports have been specifically dedicated to the linkage between the optical properties of CuPc materials to their dielectric properties, which will be important in understanding the charge transport mechanisms operative in the system. Therefore, the ground and excited state dynamics of the amorphous hyperbranched CuPc polymer systems have been extensively investigated to get a better understanding of the details of excitation and charge transport mechanisms behind the unusual dielectric behavior.

Figure 7 shows the steady-state absorption and emission of the HBCuPc-TPA-CN polymer and HBCuPc polymer. Both hyperbranched polymers showed characteristic B and Q bands for absorption of CuPc.⁶³ For the HBCuPc-TPA-CN polymer, the absorption at UV range may be assigned to C (270 nm, $d-\pi^*$), N (347 nm, $d-\pi$), and B (363 nm, $\pi-\pi^*$) bands of the CuPc ring, respectively. The strong peak at 302 nm corresponds to the absorption of the TPA moiety. The maximum B band absorption peak of HBCuPc-TPA-CN polymer showed a bathochromic shift from that of the HBCuPc polymer ($\Delta\lambda_{\max} = 27 \text{ nm}$), along with the increased intensity of the B band. It suggests that the introduction of TPA moiety may increase the conjugation part in HBCuPc-TPA-CN branch and reduces $\pi-\pi^*$ transition energy. If we compare the lower energy onset of the absorption bands of the two hyperbranched CuPc polymer systems, it appears that the HBCuPc-TPA-CN polymer may have a longer conjugation length due to the low energy onset ($E_g = 1.48 \text{ eV}$). On the basis of our previous investigations on hyperbranched materials for high

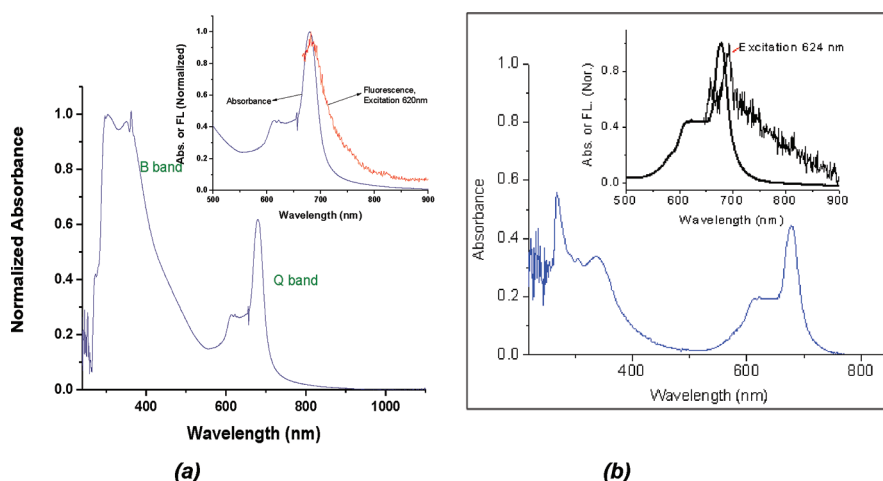


Figure 7. Absorption and emission (excitation at Q_y band) spectra of HBCuPc-TPA-CN polymer (a) and HBCuPc polymer. Part b reproduced from ref 63.

dielectric applications, one advantageous aspect was that the dielectric response will be enhanced through long-range delocalization over the molecular chain and close face-to-face packing through the intramolecular assembly. We did see the enhanced dielectric response due to this effect in comparison with linear analogues.¹ However, the strong Coulombic coupling through the donor–acceptor interaction may prohibit effective polaron hopping in the system and result in a slightly decreased dielectric constant thereafter.

The absorption peaks shown at both 622 and 680 nm were assigned to Q band ($\pi-\pi^*$) transitions. A weak emission was observed when excited at the Q_y band of 622 nm (Figure 7a inset). However, a stronger emission was observed at an excitation of ~ 400 nm, in contrast to the zero emission observed for the HBCuPc polymer. It indicates that this emission is associated with the presence of the TPA unit, and the internal conversion from S₂ to S₁ is slower in the HBCuPc-TPA-CN polymer; thus, the fluorescence is detected from both B and Q band excitation. In addition, the fluorescence peak in the red region shifts to the blue region when the excitation wavelength is changed from 622 to 400 nm, indicating that this observed red fluorescence is mainly from the second excited singlet state (S₂) and is short-lived. The emission spectrum was distorted from the mirror image of the absorption spectrum, possibly related to other nonradiative charge transfer processes, which may involve the ring-to-ring charge transfer process.

Figure 8 shows the steady-state absorption and fluorescence of diluted HBCuPc-TPA-CN sample in DMAc with an excitation of 310 nm. The strong absorption peak at 298 nm is indicative of the existence of TPA unit, and it appears very close to that of the TPA monomer (296 nm) reported. However when we excited close to the absorption peak of TPA, no fluorescence trace from TPA was detected. In addition, a Stokes shift (8847 cm^{-1}) larger than that of the HBCuPc system also indicated that the charge transfer states originated from the TPA.

Femtosecond spectroscopy has been a very powerful tool for investigating the photophysics of polymer systems. In many π -conjugated organic materials, up-converted ultrafast fluorescence dynamics and anisotropy decay experiments have been applied successfully to reveal possible ultrafast processes, such as vibrational relaxation and singlet–singlet annihilation, occurring in a

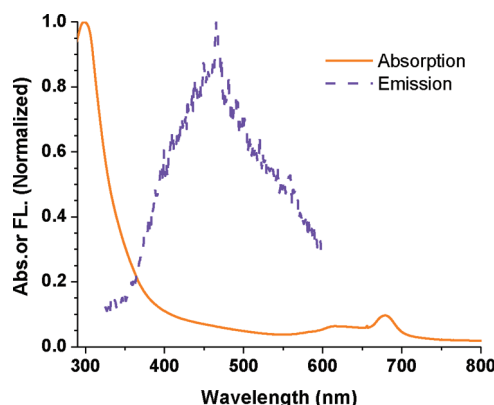


Figure 8. Steady-state absorption and fluorescence of diluted HBCuPc-TPA-CN polymer sample with an excitation at 310 nm.

time scale shorter than 20 ps, and to validate the presence and type of intramolecular energy and charge transfer processes.^{63,95–98} Recently, several reports have been published on the Q state and B state fluorescence dynamics of porphyrin derivatives by means of femtosecond fluorescence up-conversion. Anais Medina et al. have confirmed an accelerated charge transfer in a triphenylamine-subphthalocyanine donor–acceptor system through femtosecond transient absorption measurement.⁹⁹

Figure 9 shows the polarized fluorescence decay of HBCuPc-TPA-CN polymer measured at 480 nm with an excitation at 400 nm: the parallel emission is in dark color and the perpendicular emission is purple. The fluorescence intensity decays were fitted with two exponentials. A fast fluorescence decay component was found on a time scale ~ 205 fs, which is larger than the instrument response function (IRF = 114 fs). In addition, the slow fluorescence decay component was on a time scale of ~ 1.5 ps, the same magnitude as that of the HBCuPc polymer (3 ps, Figure 10), which is common to polaron hopping systems. It has been reported that the incorporation of TPA unit to the core will induce fluorescence quenching, and a fast decay is expected. In our case, about 10 times smaller quantum yield (0.0003 versus 0.004 for HBCuPc polymer) was observed in the HBCuPc-TPA-CN polymer. However, there is a very long tail after initial decay in this system, which may be due to a long lifetime of

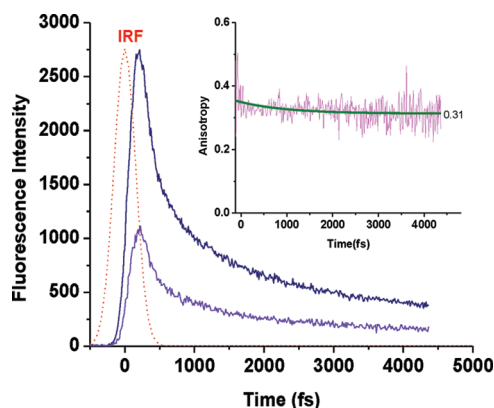


Figure 9. Up-converted fluorescence dynamics of HBCuPc-TPA-CN polymer (the inset is the anisotropy decay of HBCuPc-TPA-CN polymer).

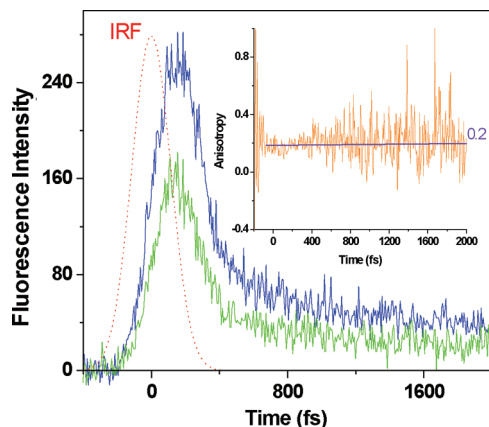


Figure 10. Up-converted fluorescence dynamics of HBCuPc polymer. Parallel emission, blue; perpendicular emission, green. The inset is the anisotropy decay of HBCuPc polymer; reproduced from ref 63.

CT state. A slower depolarization process in a time scale of ~ 3 ps was also observed in this system. This slow component may be related to the transfer of excitations from the mostly delocalized TPA to the CuPc core via a typical Föster hopping mechanism.

The HBCuPc polymer showed only a very weak fluorescence emission at 480 nm, but the emission of HBCuPc-TPA-CN polymer was stronger at the same wavelength and should be attributed to the presence of triphenylamine, which also has been found in several triphenylamine-based systems.^{100,101} We also carried out two-photon absorption measurement of both hyperbranched CuPc systems at different excitation wavelengths (730 nm–890 nm), and the two-photon cross section (δ) of HBCuPc-TPA-CN polymer is at least 10 times larger than that of the HBCuPc polymer at the same excitation wavelength (e.g., at an excitation of 850 nm, $\delta_{\text{HBCuPc-TPA-CN}} = 21$ GM and $\delta_{\text{HBCuPc}} = 1.4$ GM). This supports the charge transfer characteristic of the involved states because generally, the formation of charge transfer states between donor and acceptor is beneficial for the enhancement of two-photon cross section.

The inset in Figure 9 depicts the anisotropy decay of the HBCuPc-TPA-CN polymer. In comparison with the residue value of 0.2 in the HBCuPc polymer shown in the Figure 10 inset,

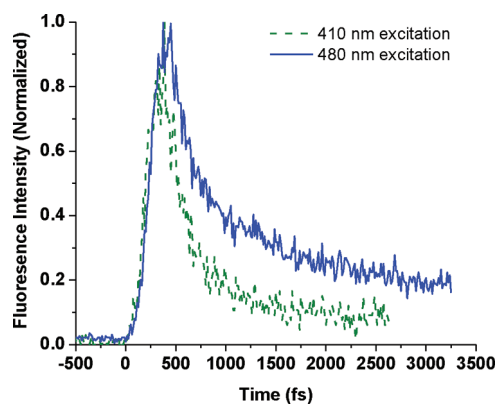


Figure 11. The up-converted fluorescence spectra of the HBCuPc-TPA-CN polymer at different excitation wavelengths (410 and 480 nm respectively).

the high residue value of ~ 0.31 is possibly due to the exciton trapping during the excited-state relaxation from the TPA unit. A similar exciton trapping phenomenon has been found in a novel triarylamine dendrimer system, in which a slow anisotropy decay in less than 100 fs occurred in the GAA-T2 dendrimer and the energy transfer phenomenon was explained by exciton trapping during the excited state relaxation process.¹⁰²

In Figure 11, we looked at the fluorescence spectra of the HBCuPc-TPA-CN polymer at different excitation wavelengths. A longer lifetime was expected for the low energy excitation, which also provides the evidence for the formation of charge transfer states between the photoexcited CuPc and TPA fragments.

To probe the nature of the excited-state interactions between the TPA moiety and CuPc core as well as to shed more light on the nature of the bathochromic shift due to the incorporation of TPA units, we also applied femtosecond transient absorption pump–probe spectroscopy. Figure 12 shows 2D transient absorption spectrum of both HBCuPc-TPA-CN and HBCuPc polymer. From the comparison of both spectra, there is an occurrence of additional charge transfer states in the HBCuPc-TPA-CN polymer because a fast decay was detected in the near-infrared region. It is possibly due to the formation of CuPc⁺–TPA⁺ charge transfer complex via an intramolecular charge transfer reaction, in accordance with what we have found from the up-conversion measurement.

Figure 13 shows the transient absorption changes ΔA as a function of wavelength with several time delays between the pump and probe pulses upon an excitation of 365 nm. It exhibits typical T_1 – T_n triplet–triplet absorption spectra of phthalocyanine compounds.^{103–105} The negative ΔA signals at 585–705 nm correspond to the photobleaching of the S_0 – S_1 transition (Q band) and correlates to the Q_v absorption band. As the time delay is increased from 200 fs to 10.2 ps, excited state absorption (ESA) with a maximum at 742 nm is slightly shifted to short wavelengths to a maximum around 739 nm. The excited state absorption was assigned to photoinduced absorption of mainly TPA⁺ cations. The maximum peak absorption is obtained at 2 ps, corresponding to the charge pair formation. Moreover, the broad, induced absorption band between 450 and 600 nm shows a blue shift as the evolution of delay time, and it could be due to the excitonic polaron state formation; that is to say, the formation of charge pair complexes. Both the absorption and photobleaching

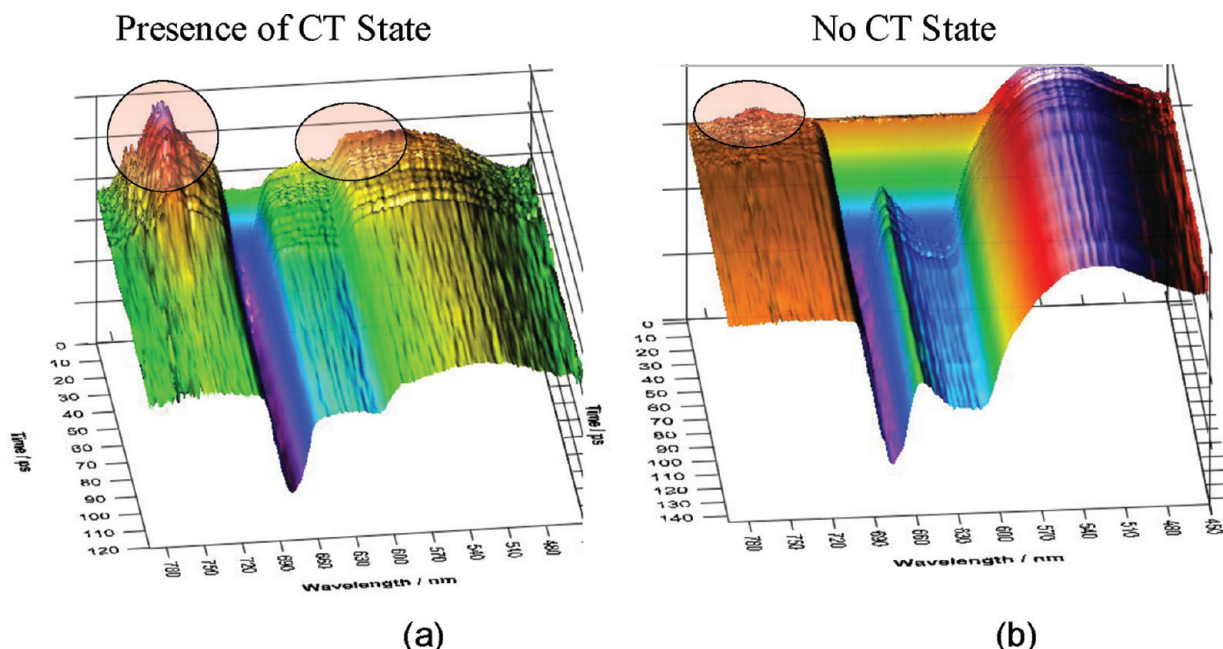


Figure 12. Transient absorption spectra of (a) HBCuPc-TPA-CN polymer and (b) HBCuPc polymer.

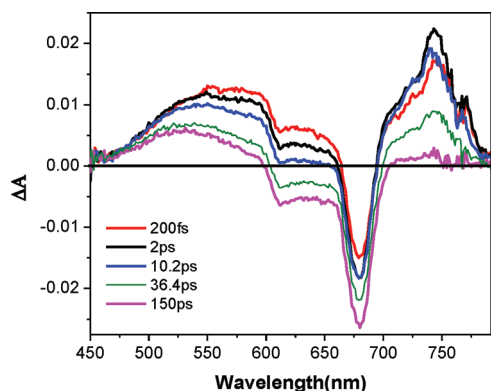


Figure 13. Transient absorption spectra at different time delays for HBCuPc-TPA-CN polymer in DMAc after excitation at 365 nm.

bands have been observed in other phthalocyanine-based polymer films and solutions.^{106,107} The weak absorption bleaching with a maximum at ~ 610 nm at 150 ps delay time could be explained by assuming a cancellation of ground state bleaching by excited state absorption or very fast localization of excitations on the molecular species with lowest excited state energy.¹⁰⁶

As observed from the global fitting of transient absorption kinetics, a decay component of 1.7 ps is observed, comparable to the slow component of fluorescence decay (\sim 1.5 ps). It suggests that polaron the hopping charge transfer mechanism is operative in the HBCuPc-TPA-CN polymer system. After 10.2 ps, the photoinduced absorption changes decreases and finally turns to a featureless peak, in accordance with the long-lived singlet state decay.

Transient spectra of principle coefficients for different time constants obtained from global fit analysis are shown in Figure 14, which concludes the complete excited state dynamics of HBCuPc-TPA-CN polymer. The faster time constant of 1.7 ps

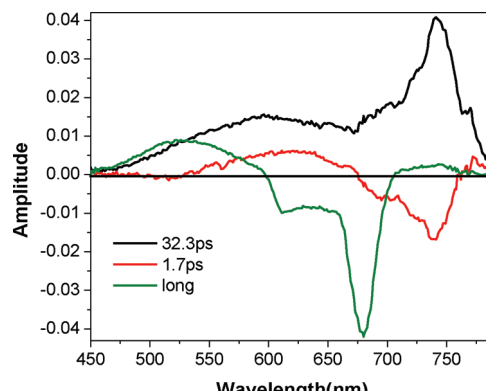


Figure 14. Transient spectra of principle coefficients at different time constants obtained from single value decomposition and consequent global fit analysis for HBCuPc-TPA-CN polymer.

is attributed to the polaron hopping. Howe et al. found a fast decay component of ~ 4 ps in a PcS_4 aqueous solution.¹⁰⁷ The time constant of 32.3 ps is ascribed from nonradiative decay from the S_1 state to the ground state in combination with intersystem crossing from S_1 to the triplet state. The excited state decaying with a long time constant (>1 ns) is ascribed to radiative decay from the S_1 state to the ground state, since the radiative decay lifetime is expected to be within nanoseconds range.¹⁰⁷

For a better comparison, we present the transient absorption spectra for HBCuPc polymer at an excitation of 365 nm (Figure 15). They show both an induced absorption band and a photobleaching band. The bleaching peaks with a maximum around 610 nm are much stronger in comparison with that in the HBCuPc-TPA-CN polymer. It can be explained by the singlet-singlet annihilation. The long wavelength absorption peaks are less pronounced in this polymer too, which suggests that stimulated absorption is less probable to occur in this system. In addition, when we look at components of HBCuPc polymer

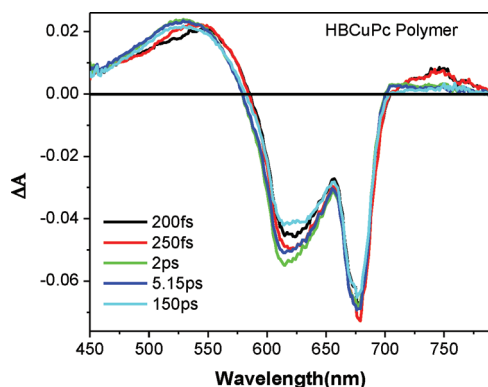


Figure 15. Transient absorption spectra at different time delays for the HBCuPc polymer in DMAc after excitation at 365 nm.

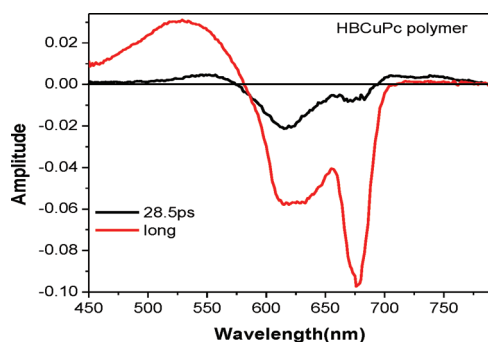


Figure 16. Transient spectra of principle coefficients at different time constants obtained from single value decomposition and consequent global fit analysis for the HBCuPc polymer.

from global fitting, as shown in Figure 16, no short time constant exists in the HBCuPc-TPA-CN polymer, and long lifetimes are similar to that of HBCuPc. The S_2 state is short-lived in this system. The conversion of the S_2 state to the S_1 state is fast, and we cannot detect it within the pulse duration (130 fs).

■ GENERAL APPLICATIONS

High dielectric constant materials are actively developed for a variety of applications:^{19,36,52,108–118} (1) High energy and high power capacitors for defibrillators, hybrid cars, pulsed plasma thrusters, and electric ships. For this application, a high dielectric constant, high breakdown voltage, and low dielectric loss are desired to provide a high and quick burst of power. Organic high dielectric constant materials will allow the cost-effective and simplified volume manufacturing with enhanced performance. (2) CMOS field effect transistors for printed circuit boards, electronic switches, and converters applications, et al., in which the device dimensions are being researched for being scaled down according to Moore's law without sacrificing the performance. The organic high dielectric materials are able to offer improved capacitance, lower leakage current, and a longer lifetime. (3) Memory storage applications. (4) Photonic band gap materials for use as microlasers, optical switches, in optical quantum computing, and as biological probes for tumor detection, et al. (5) Smart skin applications, including radar-absorbing materials and microelectromechanical systems.

■ CONCLUSIONS AND OUTLOOK

We have discussed the principle of synthesis methods for hyperbranched phthalocyanine-based polymers. This one-step synthesis method is beneficial for the scale-up of the material production for larger industrial manufacturing needs. Because cost is an important factor under consideration in competing with existing high dielectric constant materials, a great amount of effort has been taken to improve the quality of materials while lowering the cost. In addition, an eco-design synthesis route has been under active development and aimed at reducing or eliminating the environmental side effects.

The key properties we are looking at in promising novel macromolecular high dielectric constant materials are a high dielectric constant (>10), low dielectric loss (<0.01), good lifetime under applied voltage, and high thermal and chemical resistance characteristics. In our research, we have successfully discovered and developed a set of hyperbranched phthalocyanine-based polymers that have satisfied a majority of the above criteria. For example, the HBCuPc polymer has shown an impressive dielectric constant (~ 46) accompanied by a very low dielectric loss (~ 0.004) at 1 MHz. This excellent combination of dielectric properties has outperformed other reported results in phthalocyanine-based monomers and polymers. The enhanced dielectric effect in hyperbranched architecture in comparison with linear polymers has been found to be due to the long-range delocalization, which was evidenced by a series of studies utilizing ultrafast spectroscopic techniques. In addition, the intensive investigations on the photophysics of such hyperbranched systems have suggested that the donor–acceptor interaction strength, the delocalization, and the architecture of the branching system play significant roles in the resulting dielectric constant of the material. For example, the introduction of the triphenylamine donor moiety into the branch and the formation of charge transfer complexes lower the dielectric constant of the material and induce more ionic feature into the system. By shifting the connecting position of CuPc rings along the branch (e.g., from the ortho to the meso position), the separation distance between two CuPc rings will be changed, which will affect the coupling strength and change the dielectric constant thereafter.

Based on the structure–function relationship drawn by connecting the dielectric, photophysical, mechanical, and microstructural characterization analysis, different designs have been implemented and tested to optimize the hyperbranched phthalocyanine system. For example, a novel donor–acceptor material based on hyperbranched CuPc systems end-capped by a cyano group involving a TPA moiety has been synthesized for the purpose of enhancing the solubility and enabling a facile film fabrication and processing.

The major contributions from our previous studies in addition to this one have been made through our systematic investigations, which convey a better understanding in the physical mechanisms underlying the excellent dielectric properties of such hyperbranched system, which is crucial for the design of future dielectrics to better answer the needs from the performance improvement requirement.

Although some recent progress has shown the promise of organic high dielectric constant materials due to their properties and versatilities, there are still some significant technique challenges facing the organic dielectrics. For example, organic dielectrics generally exhibited a comparatively lower dielectric constant relative to inorganic dielectrics, even though the low dielectric loss has helped to compensate for this disadvantage. In addition, some organic dielectrics are thermally stable only up to their glass transition temperatures, lower than the decomposition

temperature of most ceramic dielectrics, which also limits the applicable operation circumstances.

Because the theory and modeling on the disordered organic materials are not mature yet, some are even contradictory to each other; hence, with the aid from our systematic experimental observations, advanced modeling tools should be built to better address the questions and later on to help to build up new organic dielectrics.

■ ASSOCIATED CONTENT

5 Supporting Information. Detailed description of the synthesis and characterization data of the HBCuPc-TPA-CN polymer and the figures showing ^1H NMR, ^{13}C NMR, IR, and DI-MS spectra of bis(4-methoxyphenyl)phenylamine, bis(4-hydroxyphenyl)phenylamine, bis((3,4-dicyanophenoxy)phenyl)phenylamine and HBCuPc-TPA-CN polymer. This material is available free of charge via the Internet at <http://pubs.acs.org>

■ AUTHOR INFORMATION

Corresponding Author

*E-mail: tgoodson@umich.edu.

■ BIOGRAPHIES



Meng Guo is currently on the research staff at the University of Michigan—Ann Arbor. She received her Ph.D. degree in Chemistry in 2009 from the University of Michigan. Her dissertation research was directed at the investigation of organic high dielectric constant materials for energy storage applications, mainly hyperbranched polymeric systems. Her research interests are in organic electronic and optic materials, ultrafast spectroscopy, and electrochemical systems.



Teruaki Hayakawa received his Ph.D. degree in 2000 from Yamagata University and joined the National Institute of Materials and Chemical Research (NIMC) of the Ministry of International Trade and Industry as a research scientist. In 2001, the National Institute of Advanced Industrial Science and Technology (AIST) was formed by reorganization, and he joined the Macromolecular Technology Research Center of AIST as a research scientist. In 2003, he moved to the Department of Organic and Polymeric Materials, Tokyo Institute of Technology, as an Assistant Professor. In 2009, he was promoted to Associate Professor in the same department. His recent research projects especially focus on the design of self-organizing polymeric materials, especially for block copolymer lithography, functional block copolymers, liquid crystalline epoxy materials, and polycondensation and living anionic and radical polymerizations. He has co-authored over 150 publications, including reviewing articles and book chapters.



Masa-aki Kakimoto is currently a professor in the Department of Organic and Polymeric materials, Graduate School of Science and Engineering, Tokyo Institute of Technology. He received his Ph.D. degree from the Tokyo Institute of Technology in 1980. After 2 years of research experience in the Sagami Central Research center, he started his independent research career as an Assistant Professor in the Department of Organic Polymeric Materials, Tokyo Institute of Technology, in 1982 and has stayed there ever since. Prof. Kakimoto's main research interests are (1) preparation of high performance polymers; (2) preparation of dendritic macromolecules; (3) materials for microelectronics; (4) organic and inorganic hybrids; and (5) materials for fuel cell technology (catalysts and membranes).



Theodore Goodson III is currently a Richard Barry Bernstein Collegiate Professor of Chemistry and the Professor of

Macromolecular Science and Engineering at the University of Michigan—Ann Arbor. He received his Ph.D. from the University of Nebraska (1996) and conducted his postdoc research at both the University of Chicago and Oxford University. He started as an Assistant Professor at Wayne State University and then moved to the University of Michigan—Ann Arbor in 2004. He is Senior Editor of *The Journal of Physical Chemistry B*. Professor Goodson's research interests focus on utilizing a number of spectroscopic techniques toward investigating the optical properties of novel organic macromolecular materials, targeting applications such as artificial light harvesting, light emitting, sensor, quantum optics, and sensors.

ACKNOWLEDGMENT

This research was supported by the Office of Naval Research (ONR) capacitor program.

REFERENCES

- (1) Guo, M.; Yan, X. Z.; Kwon, Y.; Hayakawa, T.; Kakimoto, M. A.; Goodson, T. *J. Am. Chem. Soc.* **2006**, *128*, 14820–14821.
- (2) Yan, X. Z.; Goodson, T. *J. Phys. Chem. B* **2006**, *110*, 14667–14672.
- (3) Zhang, Q. M.; Li, H. F.; Poh, M.; Xia, F.; Cheng, Z. Y.; Xu, H. S.; Huang, C. *Nature* **2002**, *419*, 284–287.
- (4) Chu, B. J.; Zhou, X.; Ren, K. L.; Neese, B.; Lin, M. R.; Wang, Q.; Bauer, F.; Zhang, Q. M. *Science* **2006**, *313*, 334–336.
- (5) MacDougall, F. W.; Ennis, J. B.; Cooper, R. A.; Bates, J.; Seal, K. In Pulsed Power Conference, 2003, Dallas, TX, June 15–18, 2003; Digest of Technical Papers. PPC-2003. 14th IEEE International 2003; Vol. 1, p 513–517.
- (6) Slenes, K. M.; Winsor, P.; Scholz, T.; Hudis, M. *IEEE Trans. Magn.* **2001**, *37*, 324–327.
- (7) *Handbook of Low and High Dielectric Constant Materials and Their Applications*; Nalwa, H. S., Ed.; Academic Press: London, UK, 1999; Vol. 1.
- (8) Cao, Y.; Irwin, P. C.; Younsi, K. *IEEE Trans. Dielectr. Electr. Insul.* **2004**, *11*, 797–807.
- (9) Amaral, F.; Rubinger, C. P. L.; Valente, M. A.; Costa, L. C.; Moreira, R. L. *J. Appl. Phys.* **2009**, *105*, 034109.
- (10) Wong, C. K.; Shin, F. G. *J. Appl. Phys.* **2005**, *97*, 034111.
- (11) Zhu, J. L.; Jin, C. Q.; Cao, W. W.; Wang, X. H. *Appl. Phys. Lett.* **2008**, *92*, 242901.
- (12) Jayanthi, S.; Kutty, T. R. N. *J. Mater. Sci.: Mater. Electron.* **2008**, *19*, 615–626.
- (13) Liu, D.; Tse, K.; Robertson, J. *Appl. Phys. Lett.* **2007**, *90*, 062901.
- (14) Bobade, S. M.; Gopalan, P.; Choi, D. K. *Jpn. J. Appl. Phys.* **2009**, *48*, 041402.
- (15) Hiltunen, J.; Seneviratne, D.; Tuller, H. L.; Lappalainen, J.; Lantto, V. *J. Electroceram.* **2009**, *22*, 395–404.
- (16) Ni, L.; Chen, X. M. *Solid State Commun.* **2009**, *149*, 379–383.
- (17) Prakash, B. S.; Varma, K. B. R. *J. Nanosci. Nanotechnol.* **2008**, *8*, 5762–5769.
- (18) Thongbai, P.; Yamwong, T.; Maensiri, S. *Appl. Phys. Lett.* **2009**, *94*, 152905.
- (19) Robertson, J. *Eur. Phys. J.: Appl. Phys.* **2004**, *28*, 265–291.
- (20) Haeni, J. H.; Irvin, P.; Chang, W.; Uecker, R.; Reiche, P.; Li, Y. L.; Choudhury, S.; Tian, W.; Hawley, M. E.; Craig, B.; Tagantsev, A. K.; Pan, X. Q.; Streiffer, S. K.; Chen, L. Q.; Kirchoefer, S. W.; Levy, J.; Schlom, D. G. *Nature* **2004**, *430*, 758–761.
- (21) Wilk, G. D.; Wallace, R. M.; Anthony, J. M. *J. Appl. Phys.* **2001**, *89*, 5243–5275.
- (22) Wilk, G. D.; Wallace, R. M.; Anthony, J. M. *J. Appl. Phys.* **2000**, *87*, 484–492.
- (23) Hao, W. T.; Zhang, J. L.; Tan, Y. Q.; Zhao, M. L.; Wang, C. L. *J. Am. Ceram. Soc.* **2011**, *94*, 1067–1072.
- (24) Dutta, P.; Biswas, S.; De, S. K. *J. Phys.: Condens. Matter* **2001**, *13*, 9187–9196.
- (25) Fattoum, A.; Arous, M.; Gmati, F.; Dhaoui, W.; Mohamed, A. B. *J. Phys. D: Appl. Phys.* **2007**, *40*, 4347–4354.
- (26) Nguema, E.; Vigneras, V.; Miane, J. L.; Mounaix, P. *Eur. Polym. J.* **2008**, *44*, 124–129.
- (27) Sakthivel, S.; Shekar, B. C.; Mangalaraj, D.; Narayandass, S. K.; Venkatachalam, S.; Prabhakaran, P. V. *Eur. Polym. J.* **1997**, *33*, 1747–1752.
- (28) Michalczyk, P.; Bramouille, M. *IEEE Trans. Magn.* **2003**, *39*, 362–365.
- (29) Singh, N. L.; Sharma, A.; Shrinet, V.; Rakshit, A. K.; Avasthi, D. K. *Bull. Mater. Sci.* **2004**, *27*, 263–267.
- (30) Bai, Y.; Cheng, Z. Y.; Bharti, V.; Xu, H. S.; Zhang, Q. M. *Appl. Phys. Lett.* **2000**, *76*, 3804–3806.
- (31) Bobnar, V.; Levstik, A.; Huang, C.; Zhang, Q. M. *Phys. Rev. Lett.* **2004**, *92*, 047604.
- (32) Clayton, L. M.; Sikder, A. K.; Kumar, A.; Cinke, M.; Meyyappan, M.; Gerasimov, T. G.; Harmon, J. P. *Adv. Funct. Mater.* **2005**, *15*, 101–106.
- (33) Dang, Z. M.; Fan, L. Z.; Shen, Y.; Nan, C. W. *Chem. Phys. Lett.* **2003**, *369*, 95–100.
- (34) Dang, Z. M.; Lin, Y. H.; Nan, C. W. *Adv. Mater.* **2003**, *15*, 1625–1629.
- (35) Dang, Z. M.; Wang, L.; Yin, Y.; Zhang, Q.; Lei, Q. Q. *Adv. Mater.* **2007**, *19*, 852–857.
- (36) Dang, Z. M.; Zhou, T.; Yao, S. H.; Yuan, J. K.; Zha, J. W.; Song, H. T.; Li, J. Y.; Chen, Q.; Yang, W. T.; Bai, J. *Adv. Mater.* **2009**, *21*, 2077–2082.
- (37) Li, Q.; Xue, Q. Z.; Zheng, Q. B.; Hao, L. Z.; Gao, X. L. *Mater. Lett.* **2008**, *62*, 4229–4231.
- (38) Lu, J.; Moon, K. S.; Wong, C. P. *J. Mater. Chem.* **2008**, *18*, 4821–4826.
- (39) Lu, J. X.; Moon, K. S.; Xu, J. W.; Wong, C. P. *J. Mater. Chem.* **2006**, *16*, 1543–1548.
- (40) Mdahri, A.; Khissi, M.; Achour, M. E.; Carmona, F. *Eur. Phys. J.: Appl. Phys.* **2008**, *41*, 215–220.
- (41) Qi, L.; Lee, B. I.; Chen, S. H.; Samuels, W. D.; Exarhos, G. J. *Adv. Mater.* **2005**, *17*, 1777–1781.
- (42) Xie, Y. C.; Yu, D. M.; Min, C.; Guo, X. S.; Wan, W. T.; Zhang, J.; Liang, H. L. *J. Appl. Polym. Sci.* **2009**, *112*, 3613–3619.
- (43) Yao, S. H.; Dang, Z. M.; Jiang, M. J.; Bai, J. *Appl. Phys. Lett.* **2008**, *93*, 182905.
- (44) Yao, S. H.; Dang, Z. M.; Xu, H. P.; Jiang, M. J.; Bai, J. *Appl. Phys. Lett.* **2008**, *92*, 082902.
- (45) Kofod, G.; Risso, S.; Stoyanov, H.; McCarthy, D. N.; Sokolov, S.; Krahnert, R. *ACS Nano* **2011**, *5*, 1623–1629.
- (46) Zhou, W. Y.; Yu, D. M. *J. Appl. Polym. Sci.* **2010**, *118*, 3156–3166.
- (47) Sun, L. L.; Li, B.; Zhao, Y.; Mitchell, G.; Zhong, W. H. *Nanochemistry* **2010**, *21*, 305702.
- (48) Guo, N.; DiBenedetto, S. A.; Tewari, P.; Lanagan, M. T.; Ratner, M. A.; Marks, T. J. *J. Chem. Mater.* **2010**, *22*, 1567–1578.
- (49) He, L. X.; Tjong, S. C. *Curr. Nanosci.* **2010**, *6*, 40–44.
- (50) Panwar, V.; Park, J. O.; Park, S. H.; Kumar, S.; Mehra, R. M. *J. Appl. Polym. Sci.* **2010**, *115*, 1306–1314.
- (51) Deng, Y.; Zhang, Y. J.; Xiang, Y.; Wang, G. S.; Xu, H. B. *J. Mater. Chem.* **2009**, *19*, 2058–2061.
- (52) Rao, Y.; Ogitani, S.; Kohl, P.; Wong, C. P. *J. Appl. Polym. Sci.* **2002**, *83*, 1084–1090.
- (53) Rao, Y.; Wong, C. P. *J. Appl. Polym. Sci.* **2004**, *92*, 2228–2231.
- (54) Lu, J. X.; Wong, C. P. *IEEE Trans. Dielectr. Electr. Insul.* **2008**, *15*, 1322–1328.
- (55) Shen, Y.; Lin, Y. H.; Nan, C. W. *Adv. Funct. Mater.* **2007**, *17*, 2405–2410.
- (56) Pecharroman, C.; Moya, J. S. *Adv. Mater.* **2000**, *12*, 294–297.
- (57) Lu, J. X.; Moon, K. S.; Kim, B. K.; Wong, C. P. *Polymer* **2007**, *48*, 1510–1516.
- (58) Wang, J. W.; Wang, Y.; Wang, F.; Li, S. Q.; Xiao, J.; Shen, Q. D. *Polymer* **2009**, *50*, 679–684.

- (59) Hartman, R. D.; Pohl, H. A. *J. Polym. Sci., Part A-1: Polym. Chem.* **1968**, *6*, 1135–1152.
- (60) Bayer, I. S.; Biswas, A.; Szczecz, J. B.; Suhir, E.; Norton, M. G. *Appl. Phys. Lett.* **2008**, *92*, 083303.
- (61) Wyhof, J. R.; Pohl, H. A. *J. Polym. Sci., Part A-2: Polym. Phys.* **1970**, *8*, 1741–1754.
- (62) Zhang, J.; Zhu, D.; Matsuo, M. *Polymer* **2008**, *49*, 5424–5430.
- (63) Guo, M.; Yan, X. Z.; Goodson, T. *Adv. Mater.* **2008**, *20*, 4167–4171.
- (64) Yan, X. Z.; Pawlas, J.; Goodson, T.; Hartwig, J. F. *J. Am. Chem. Soc.* **2005**, *127*, 9105–9116.
- (65) Ranasinghe, M. I.; Varnavski, O. P.; Pawlas, J.; Hauck, S. I.; Louie, J.; Hartwig, J. F.; Goodson, T. *J. Am. Chem. Soc.* **2002**, *124*, 6520–6521.
- (66) Ramakrishna, G.; Goodson, T. *J. Phys. Chem. A* **2007**, *111*, 993–1000.
- (67) Voit, B. I.; Lederer, A. *Chem. Rev.* **2009**, *109*, 5924–5973.
- (68) Kitajyo, Y.; Kinugawa, Y.; Tamaki, M.; Kaga, H.; Kaneko, N.; Satoh, T.; Kakuchi, T. *Macromolecules* **2007**, *40*, 9313–9321.
- (69) Hao, J. J.; Jiikei, M.; Kakimoto, M. A. *Macromolecules* **2002**, *35*, 5372–5381.
- (70) Emrick, T.; Chang, H. T.; Frechet, J. M. J. *Macromolecules* **1999**, *32*, 6380–6382.
- (71) Gao, C.; Yan, D. Y. *Macromolecules* **2001**, *34*, 156–161.
- (72) Rannard, S. P.; Davis, N. J. *J. Am. Chem. Soc.* **2000**, *122*, 11729–11730.
- (73) Frechet, J. M. J.; Henmi, M.; Gitsov, I.; Aoshima, S.; Leduc, M. R.; Grubbs, R. B. *Science* **1995**, *269*, 1080–1083.
- (74) Sakamoto, K.; Aimiya, T.; Kira, M. *Chem. Lett.* **1997**, 1245–1246.
- (75) Carlmark, A.; Hawker, C. J.; Hult, A.; Malkoch, M. *Chem. Soc. Rev.* **2009**, *38*, 352–362.
- (76) Yates, C. R.; Hayes, W. *Eur. Polym. J.* **2004**, *40*, 1257–1281.
- (77) Gao, C.; Yan, D. *Prog. Polym. Sci.* **2004**, *29*, 183–275.
- (78) Jiikei, M.; Kakimoto, M. *Prog. Polym. Sci.* **2001**, *26*, 1233–1285.
- (79) Voit, B. *J. Polym. Sci., Part A: Polym. Chem.* **2000**, *38*, 2505–2525.
- (80) Kwon, Y.; Hayakawa, T.; Kakimoto, M. A. *Chem. Lett.* **2006**, *35*, 1306–1307.
- (81) Lee, T. K., Y.; Park, J. J.; Pu, L.; Hayakawa, T.; Kakimoto, M. A. *Macromol. Rapid Commun.* **2007**, 1657–1662.
- (82) Liaw, D. J.; Hsu, P. N.; Chen, W. H.; Lin, S. L. *Macromolecules* **2002**, *35*, 4669–4676.
- (83) Kohler, A.; Bassler, H. *Mater. Sci. Eng. Rep.* **2009**, *66*, 71–109.
- (84) Karabunarliev, S.; Bittner, E. R. *Phys. Rev. Lett.* **2003**, *90*, 057402.
- (85) Westenhoff, S.; Howard, I. A.; Hodgkiss, J. M.; Kirov, K. R.; Bronstein, H. A.; Williams, C. K.; Greenham, N. C.; Friend, R. H. *J. Am. Chem. Soc.* **2008**, *130*, 13653–13658.
- (86) Segal, M.; Singh, M.; Rivoire, K.; Difley, S.; Van Voorhis, T.; Baldo, M. A. *Nat. Mater.* **2007**, *6*, 374–378.
- (87) Bobnar, V.; Levstik, A.; Huang, C.; Zhang, Q. M. *J. Non-Cryst. Solids* **2007**, *353*, 205–209.
- (88) Gould, R. D. *Coord. Chem. Rev.* **1996**, *156*, 237–274.
- (89) Sakai, Y.; Sadaoka, Y.; Yokouchi, H. *Bull. Chem. Soc. Jpn.* **1974**, *47*, 1886–1888.
- (90) Vidadi, Yu. A.; Rozenshtein, L. D.; Chistyakov, E. A. *Sov. Phys. Solid State* **1969**, *17*.
- (91) Kiess, H.; Rehwald, W. *Colloid Polym. Sci.* **1980**, *258*, 241–251.
- (92) Pelster, R.; Nimtz, G.; Wessling, B. *Phys. Rev. B* **1994**, *49*, 12718–12723.
- (93) Wang, Z. H.; Scherr, E. M.; Macdiarmid, A. G.; Epstein, A. J. *Phys. Rev. B* **1992**, *45*, 4190–4202.
- (94) Martens, H. C. F.; Brom, H. B. *Physical Review B* **2004**, *70*, 241201.
- (95) Guo, M.; Varnavski, O.; Narayanan, A.; Mongin, O.; Majoral, J. P.; Blanchard-Desce, M.; Goodson, T. *J. Phys. Chem. A* **2009**, *113*, 4763–4771.
- (96) Varnavski, O.; Bauerle, P.; Goodson, T. *Opt. Lett.* **2007**, *32*, 3083–3085.
- (97) Cannizzo, A.; Blanco-Rodriguez, A. M.; El Nahhas, A.; Sebera, J.; Zalis, S.; Vlcek, A.; Chergui, M. *J. Am. Chem. Soc.* **2008**, *130*, 8967–8974.
- (98) Muller, J. G.; Atas, E.; Tan, C.; Schanze, K. S.; Kleiman, V. D. *J. Am. Chem. Soc.* **2006**, *128*, 4007–4016.
- (99) Medina, A. S.; Claessens, C. G.; Rahman, G. M. A.; Lamsabhi, A. M.; Mo, O.; Yanez, M.; Guldi, D. M.; Torres, T. *Chem. Commun.* **2008**, 1759–1761.
- (100) D'Souza, F.; Gadde, S.; Islam, D. M. S.; Wijesinghe, C. A.; Schumacher, A. L.; Zandler, M. E.; Araki, Y.; Ito, O. *J. Phys. Chem. A* **2007**, *111*, 8552–8560.
- (101) Huang, C. W.; Chiu, K. Y.; Cheng, S. H. *Dalton Trans.* **2005**, 2417–2422.
- (102) Hagedorn, K. V.; Varnavski, O.; Hartwig, J.; Goodson, T. *J. Phys. Chem. C* **2008**, *112*, 2235–2238.
- (103) Zhang, X. F.; Di, Y. Q.; Zhang, F. S. *J. Photochem. Photobiol. A* **2009**, *203*, 216–221.
- (104) Ohkubo, K.; Fukuzumi, S. *J. Porphyrins Phthalocyanines* **2008**, *12*, 993–1004.
- (105) Martin-Gomis, L.; Ohkubo, K.; Fernandez-Lazaro, F.; Fukuzumi, S.; Sastre-Santos, A. *J. Phys. Chem. C* **2008**, *112*, 17694–17701.
- (106) Gulbinas, V.; Chachisvilis, M.; Valkunas, L.; Sundstrom, V. *J. Phys. Chem.* **1996**, *100*, 2213–2219.
- (107) Howe, L.; Zhang, J. *Z. J. Phys. Chem. A* **1997**, *101*, 3207–3213.
- (108) Kim, C.; Wang, Z. M.; Choi, H. J.; Ha, Y. G.; Facchetti, A.; Marks, T. J. *J. Am. Chem. Soc.* **2008**, *130*, 6867–6878.
- (109) Ortiz, R. P.; Facchetti, A.; Marks, T. J. *Chem. Rev.* **2010**, *110*, 205–239.
- (110) Dimitrakopoulos, C. D.; Purushothaman, S.; Kymmissis, J.; Callegari, A.; Shaw, J. M. *Science* **1999**, *283*, 822–824.
- (111) Homes, C. C.; Vogt, T.; Shapiro, S. M.; Wakimoto, S.; Ramirez, A. P. *Science* **2001**, *293*, 673–676.
- (112) Carlson, C. M.; Rivkin, T. V.; Parilla, P. A.; Perkins, J. D.; Ginley, D. S.; Kozyrev, A. B.; Oshadchy, V. N.; Pavlov, A. S. *Appl. Phys. Lett.* **2000**, *76*, 1920–1922.
- (113) Scott, J. F. *Annu. Rev. Mater. Sci.* **1998**, *28*, 79–100.
- (114) Kotecki, D. E. *Integr. Ferroelectr.* **1997**, *16*, 1–19.
- (115) Pelrine, R.; Kornbluh, R.; Kofod, G. *Adv. Mater.* **2000**, *12*, 1223–1225.
- (116) Jiang, S. L.; Yu, Y.; Zeng, Y. K. *Curr. Appl. Phys.* **2009**, *9*, 956–959.
- (117) Raval, H. N.; Tiwari, S. P.; Navan, R. R.; Mhaisalkar, S. G.; Rao, V. R. *IEEE Electron Device Lett.* **2009**, *30*, 484–486.
- (118) Khan, M. Z. R.; Hasko, D. G.; Saifullah, M. S. M.; Welland, M. E. *J. Phys. Condens. Matter* **2009**, *21*, 215902.